Fabrication of Fine Zeolite with Improved Catalytic Properties by Bead Milling and Alkali Treatment

Toru Wakihara,* Koki Sato, Satoshi Inagaki, Junichi Tatami, Katsutoshi Komeya, Takeshi Meguro, and Yoshihiro Kubota

Graduate School of Environment and Information Sciences, Yokohama National University, 79-7 Tokiwadai, Hodogaya-ku, Yokohama 240-8501, Japan

ABSTRACT Zeolites with high external surface area allow diffusing reactants greater access to catalytically active sites, which has lead to interest in the preparation of nano-zeolites. In this study, a top-down approach has been used, first milling the zeolite to produce a fine powder. This technique can cause destruction of the outer portion of the zeolite framework, which deactivates the catalyst. To remedy this, the damaged part was removed using an alkaline solution after bead milling treatment. As a result, the designed zeolite powder yielded almost twice the amount of benzene compared with the raw zeolite when cumene was cracking into benzene and propylene.

KEYWORDS: zeolite • catalytic • milling • ZSM-5 • cracking • desilication

Zeolites are hydrated, crystalline tectoaluminosilicate structures, formed from TO_4 tetrahedra (T = tetrahedral atom, e.g., Si or Al). Their structures contain nanometer-sized and well-ordered void spaces and have been used as catalysts, ion exchangers, adsorbents, and molecular-sieving membranes, among other uses (1, 2). Currently, there are massive efforts being made into the synthesis of new kinds of zeolite and related materials for catalytic applications (3). Modification methods of zeolite have been especially productive in the optimization of catalytic processes (4–6). Recently, preparations of zeolites with high external surface area (7) by post-synthesis treatment (5, 6, 8, 9) and by the synthesis of nano-zeolites (10–13) have been the focus of much attention. Zeolites with high external surface areas allow for greater diffusion of reactants and allow reactants easier access to the catalytically active sites. This is one of the reasons for a higher catalytic activity in some zeolites, because diffusion through the zeolite pore structure is often the rate-determining step of a catalytic reaction (14). For example, Ogura et al. reported that the alkali treatment (desilication) of ZSM-5 formed mesopores that were uniform in size without any change in the microporous structure and that they showed a higher catalytic reactivity than the unmodified ZSM-5 (6). In the study presented here, milling was used as a breakdown approach (15, 16) for the fabrication of fine zeolites. Conventional milling methods such as ball-milling and planetary ball-milling do improve catalytic activity; however, destruction of the outer zeolite framework causes pore blocking, and this impedes catalysis (17). Therefore, a milder milling method is required to fabricate fine zeolites without destroying crystallinity. Bead milling in particular suppresses damage to the target powder, e.g., amorphization and/or formation of dislocations, by the use of small beads 30−500 μm in diameter (see the Supporting Information), and it is possible to prepare large-scale amounts of fine zeolite without the use of a specific organic compound to control zeolite nucleation and crystal growth. Previous studies have reported zeolites that have been properly pulverized give better catalytic properties (18–20); however, it is still difficult to prevent damage to the zeolite structure even if bead milling is used. In this study, therefore, the damaged part has been removed after bead milling using an alkaline solution as shown in the Scheme 1, and its catalytic ability has been compared with the original zeolite.

Scheme 1. Schematic Illustration Describing the Fabrication Process of Fine Zeolite by Bead Milling and Post-Milling Alkali Treatment

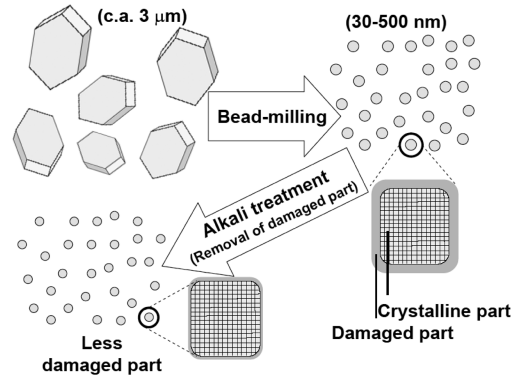

Commercial ZSM-5 (MFI type zeolite, Si/Al = 19.7, Cation: NH_4^+. 840NHA Tosoh Co., Japan) was used in this study (Zraw). The raw ZSM-5 was milled using a bead milling

* Corresponding author. Tel: +81-45-339-3957. Fax: +81-45-339-3957. E-mail: wakihara@ynu.ac.jp.
Received for review July 21, 2010 and accepted September 9, 2010

DOI: 10.1021/am100642w

apparatus (Minicer, Ashizawa Finetech Ltd., Japan). Sixty grams of ZSM-5 was dispersed in 350 mL of ethanol using an ultrasonic vibrator (VCX 600, Sonic & Materials Inc., USA) and the slurry was pulverized for 60 and 120 min using zirconia beads 300 μm in diameter. An agitation speed of 3000 rpm was used to exert both shearing and imparting force on the ZSM-5 agglomerates. After milling, the slurries were dried overnight in an oven at 373 K. These materials were designated as Z60 and Z120, respectively. Alkali treatment of the ZSM-5 zeolite was performed with aqueous solutions of 0.5M NaOH. First, 100 mL of the aqueous solution was heated to 313 K using an oil bath. Then, 3 g of zeolite, either Zraw, Z60, or Z120, was added to the heated solution with stirring. After a period of 30 min at 313 K, the slurry was then centrifuged and the supernatant liquid was decanted off. The residual solid was washed with distilled water several times. These samples obtained were designated as Zraw-AT, Z60-AT, and Z120-AT, respectively. The phases present and the morphology of the products were identified by conventional X-ray diffractometry (XRD, Multiflex, Rigaku, Tokyo, Japan) and field emission scanning electron microscopy (FE-SEM, S-5200, Hitachi, Tokyo, Japan). The crystallinity of ZSM-5 was estimated according to the following equation

$$\alpha\,(\%) = \frac{\text{peak area } 2\theta\ 22\ -\ 25^\circ \text{ for the product}}{\text{peak area } 2\theta\ 22\ -\ 25^\circ \text{ for Zraw}} \times 100 \quad (1)$$

The alkali-treated ZSM-5 zeolites were obtained in a Na-exchanged form, so that they were ion-exchanged into NH_4^+ form prior to the investigation of their catalytic performance (6). Cumene cracking into benzene and propylene was conducted in a pulse-injection flow reactor connected to an on-line TCD gas chromatograph (GC-6A, Shimadzu, Tokyo, Japan) as shown in the Supporting Information. First, 10 mg of the zeolite sample was pretreated at 673 K for 1 h to remove NH_3 and obtain H-ZSM-5. Then, the temperature of the catalyst bed was kept at 523 K and 1 μl of cumene was injected into the He carrier gas (25 $cm^3\ min^{-1}$). The benzene yield was used as an estimate of the apparent catalytic activity of each sample. Nitrogen adsorption and desorption measurements (Autosorb-1, Quantachrome, USA) were also performed at liquid nitrogen temperature (77 K). The sample was degassed in vacuum at 573 K prior to measurement. The total surface area was calculated according to the Brunauer-Emmet-Teller (BET) isothermal equation. The external surface area was also evaluated by the *t*-plot method (21). Note that the compositions of all samples were measured using X-ray fluorescence spectrometry (XRF, JSX-3202, JEOL, Tokyo, Japan) and no changes were seen in the Si/Al ratios throughout the treatments.

Typical FE-SEM images of ZSM-5 samples are shown in Figure 1. The raw zeolite has smooth morphological features. After bead milling the ZSM-5 the morphology has changed dramatically. The raw zeolite (average: 3 μm) became particles about 50−500 nm (average 170 nm) and 30−300 nm (average 70 nm) after bead milling for 60 and 120 min,

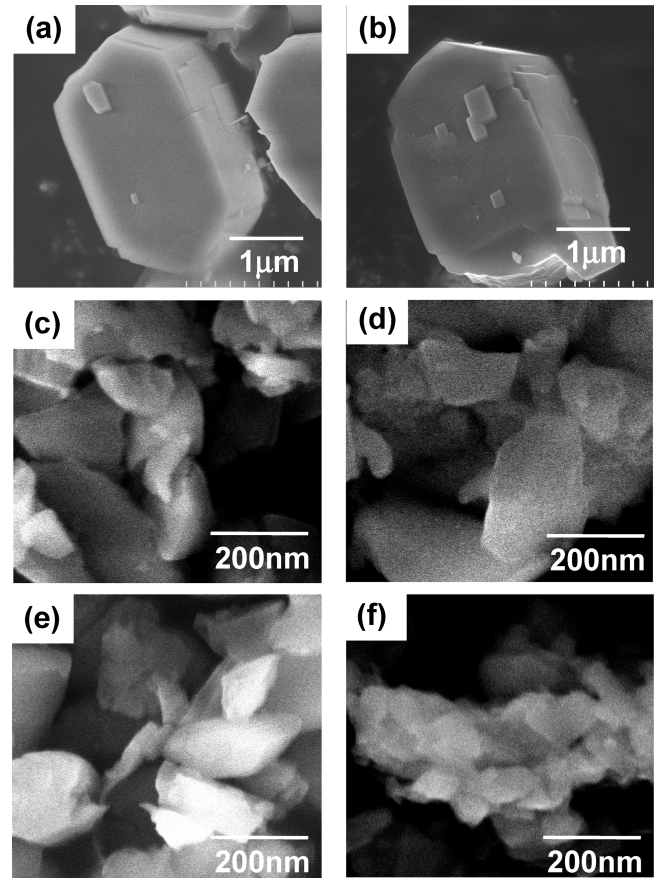

FIGURE 1. FE-SEM images of samples. (a) Zraw, (b) Zraw-AT, (c) Z60, (d) Z60-AT, (e) Z120, and (f) Z120-AT, respectively.

Table 1. Weight Ratio after Alkali Treatment, Crystallinity, BET Surface Area, and Catalytic Activities of Samples for Cumene Cracking

sample	recovery ratio (%)	crystallinity α (%)	BET surface area, S_{BET} ($m^2\ g^{-1}$)	benzene yield (%)[a]
Zraw		100	421	29
Z60		66	340	42
Z120		41	259	29
Zraw-AT	93	100	429	36
Z60-AT	65	75	430	59
Z120-AT	45	63	419	44

[a] Details are shown in the Supporting Information.

respectively. Table 1 shows the weight changes of Zraw-AT, Z60-AT and Z120-AT after alkali-treatment. 65 and 45% of the zeolites were recovered after alkali treatment for Z60-AT and Z120-AT, respectively. A previous study reported the mesopores which were created by the alkali treatment of ZSM-5 were uniform in size (6); however, these results could not be confirmed in any of the samples treated here (Zraw-AT, Z60-AT, and Z120-AT). This difference may be due to the differences in the alkali treatment (e.g. concentration of NaOH, temperature, treatment period, etc). The XRD patterns of the samples are shown in Figure 2. The crystallinity of the samples was estimated from the XRD peak areas, which are also shown in Table 1. The diffraction peaks assigned to an MFI structure showed that the structure was

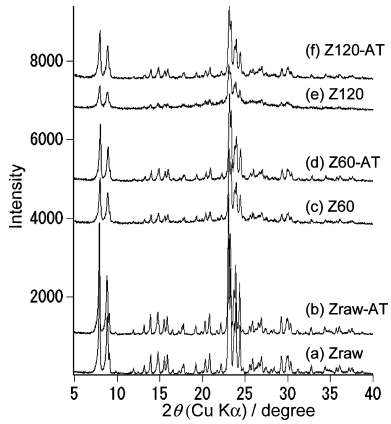

FIGURE 2. XRD patterns of samples: (a) Zraw, (b) Zraw-AT, (c) Z60, (d) Z60-AT, (e) Z120, and (f) Z120-AT, respectively. (e) All Bragg peaks seen in the samples are due to MFI structure. Patterns b−f are offset vertically by 1000, 3800, 4900, 6700, and 7500, respectively, for clarity.

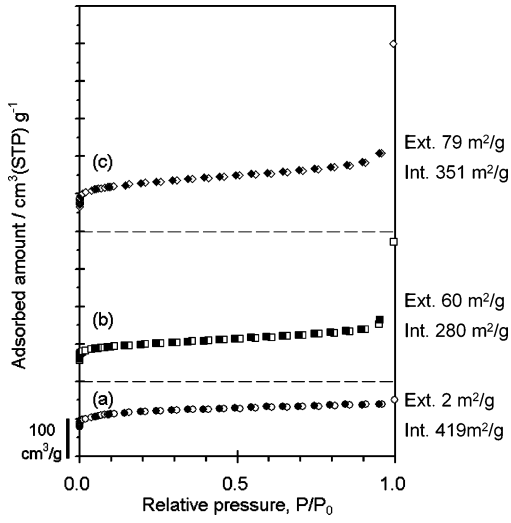

FIGURE 3. Nitrogen adsorption-desorption isotherms of (a) as-received ZSM-5 (Zraw), (b) ZSM-5 milled for 60 min (Z60), and (c) ZSM-5 milled for 60 min and with alkaline treatment (Z60-AT). To allow for a better comparison, the data for b and c were shifted by 200 and 600 $cm^3(STP)\ g^{-1}$, respectively. On the right, external (Ext.) and internal (Int.) surface areas of the samples as evaluated by *t*-plot method are also shown. Note that the external surface area of Zraw is an estimated value based on the particle size.

maintained through the milling and alkali treatments. The peak intensities in bead milled samples gradually decreased with milling, indicating an increase in damage to the crystallinity. On the other hand, the peak intensity of the ZSM-5 improved after the alkali treatment. It appears that the poorly crystalline parts of the ZSM-5 are more easily dissolved than the crystalline parts. This increases the fraction of crystalline zeolite after the alkali treatment as shown in Table 1 (Z60(66%) → Z60-AT(75%), Z120(41%) → Z120-AT(63%)).

Nitrogen adsorption and desorption isotherms of Zraw, Z60, and Z60-AT, respectively, are shown in Figure 3 to confirm the lack of formation of mesopores by alkali treatment as mentioned in the previous study (6). The initial slope of the isotherm corresponds to adsorption in the microstructure of the zeolite and was barely changed by the milling and alkali treatments. Furthermore, a hysteresis loop does not appear in the Z60-AT data, indicating mesopores have not been formed by alkali treatment. This is supported by the previous report that the desilication method is efficient when the Si/Al ratio of a zeolite is ca. 25−50 (22) (In the present study, the Si/Al ratio of Zraw is 19.7). BET surface areas of the samples are also summarized in Table 1. The BET surface areas of Z60 and Z120 were lower than the original value (Zraw), while those of Z60-AT and Z120-AT were similar to Zraw. It is assumed that the amorphous part formed by bead milling has less or no contribution to the N_2 adsorption and, as a result, the BET surface areas were decreased as the milling period increased. On the other hand, as alkali treatment removes the low crystallinity part formed by bead milling, leaving fine zeolite particles with BET surface areas similar to Zraw. Note that the less crystalline parts have not been perfectly removed even after alkali treatment. BET surface areas are a total of internal and external surface areas and the internal surface area of the alkali treated samples are still lower than that of Zraw as shown in Figure 3. This also implies Z60-AT has a lower crystallinity than that of Zraw as shown in Table 1.

All samples were evaluated as acid catalysts for cumene cracking. The measurements were conducted such that diffusion through the zeolite pore structure was the rate-determining step of a catalytic reaction (6). The results are summarized in Table 1. Over 10 pulses of cumene, the catalytic activity of all the catalysts declined only slightly and the benzene yield of the first pulses are summarized in Table 1. In these standard conditions, the conversion for Zraw was 29%. After alkali treatment, Zraw-AT (36%) had a slightly higher conversion than Zraw; indicating that diffusion was promoted by the dissolution of low crystallinity parts of the zeolite, such as dislocations, even though this kind of pore formation was not confirmed by FE-SEM as shown in Figure 1b. The benzene yield is dramatically increased by bead milling for 60 min (42%), but decreased after 120 min milling (29%). This can be explained as the bead milling promotes the formation of finer zeolite particles and hence the conversion of cumene into benzene; but too much milling causes damage to the crystallinity, which in turn lowers the catalytic activity. From these results, it can be deduced that proper bead milling treatment of zeolite is effective in improving the catalytic activity. On the other hand, the catalytic property was significantly improved in the samples obtained from the post-milling alkali treatment (Z60(42%) → Z60-AT(59%), Z120(29%) → Z120-AT(44%)). This appears to be due to the dissolution of poor crystallinity parts formed by the bead milling. Z60-AT showed a higher conversion ratio than Z120-AT. Since there is almost no change in the acid strength originating from the zeolitic nature of the raw, milled, and alkali treated zeolites (see the Supporting Information), the higher conversion ratio of Z60-AT appears to be due to its higher crystallinity than Z120-AT as shown in Table 1. It appears that the catalytic properties are therefore determined by a balance between the particle size and degree of crystallinity. In this study, by the combination of bead milling and post-milling alkali

treatment, specifically for the Z60-AT sample showed almost twice the catalytic activity of Zraw.

In conclusion, the catalytic properties of a zeolite have been improved using a combination of bead milling and post-milling alkali treatment for the first time. Bead milling clearly promotes the formation of fine zeolite particles and hence the conversion of cumene into benzene. Too much milling, however, causes damage to the crystallinity, which in turn lowers the catalytic activity. To remedy this, the damaged part of the zeolite can be removed using an alkaline solution after bead milling treatment, and as a result, the zeolite powder showed almost twice the yield of benzene than the raw zeolite. Although the desilication is performed at the expense of substantial loss of crystalline material and will have limited efficiency in certain zeolites (22), the present method makes it possible to produce a fine zeolite without using specific organic compounds to control zeolite nucleation and crystal growth and is applicable to large-scale production of zeolite. Further studies on the optimization of the conditions for bead milling and post-milling alkali treatment of other zeolites will be published elsewhere.

Acknowledgment. The authors thank Profs. T. Tatsumi and T. Yokoi from the Tokyo Institute of Technology for FE-SEM measurements.

Supporting Information Available: Temperature-programmed desorption (TPD) profiles of ammonia, and schematic drawings of bead milling and cumene cracking (PDF). This material is available free of charge via the Internet at http://pubs.acs.org.

REFERENCES AND NOTES

(1) Cundy, C. S.; Cox, P. A. *Chem. Rev.* **2003**, *103*, 663.
(2) Wakihara, T.; Okubo, T. *Chem. Lett.* **2005**, *34*, 276.
(3) Davis, M. E.; Zones, S. I. In *Synthesis of Porous Materials: Zeolites, Clays and Nanostructures*; Occelli, M. L., Kesseler, H., Eds.; Marcel Dekker: New York, 1996.
(4) Camblor, M. A.; Villaescusa, L. A.; Diaz-Cabanas, M. J. *Topics Catal.* **1999**, *9*, 59.
(5) Ogura, M.; Shinomiya, S.; Tateno, J.; Nara, Y.; Kikuchi, E.; Matsukata, M. *Chem. Lett.* **2000**, 882.
(6) Ogura, M.; Shinomiya, S.; Tateno, J.; Nara, Y.; Nomura, M.; Kikuchi, E.; Matsukata, M. *Appl. Catal. A* **2001**, *219*, 33.
(7) Gu, L.; Ma, D.; Yao, S.; Wang, C.; Shen, W.; Bao, Z. *Chem Commun.* **2010**, *46*, 1733.
(8) Groen, J. C.; Moulijn, J. A.; Perez-Ramirez, J. *J. Mater. Chem.* **2006**, *16*, 2121.
(9) Groen, J. C.; Bach, T.; Ziese, U.; Donk, A. M. P. V.; de Jong, K. P.; Moulijn, J. A.; Perez-Ramirez, J. *J. Am. Chem. Soc.* **2005**, *127*, 10792.
(10) Fan, W.; Snyder, M. A.; Kumar, S.; Lee, P. S.; Yoo, W. C.; McCormick, A. V.; Penn, R. L.; Stein, A.; Tsapatsis, M. *Nat. Mater.* **2008**, *7*, 984.
(11) Choi, M.; Na, K.; Kim, J.; Sakamoto, Y.; Terasaki, O.; Ryoo, R. *Nature* **2009**, *461*, 246.
(12) Mintova, S.; Olson, N. H.; Valtchev, V.; Bein, T. *Science* **1999**, *283*, 958.
(13) Tosheva, L.; Valtchev, V. P. *Chem. Mater.* **2005**, *17*, 2494.
(14) Sato, K.; Nishimura, Y.; Shimada, H. *Catal. Lett.* **1999**, *60*, 83.
(15) Belaroui, K.; Pons, M. N.; Vivier, H.; Meijer, M. *Powder Technol.* **1999**, *105*, 396.
(16) Valtchev, V.; Mintova, S.; Dimov, V.; Toneva, A.; Radev, D. *Zeolites* **1995**, *15*, 193.
(17) Kharitonov, A. S.; Fenelonov, V. B.; Voskresenskaya, T. P.; Rudina, N. A.; Molchanov, V. V.; Plyasova, L. M.; Panov, G. I. *Zeolites* **1995**, *15*, 253.
(18) Akcay, K.; Sirkecioglu, A.; Tatlier, M.; Savasci, O. T.; Erdem-Senatalar, A. *Powder Technol.* **2004**, *142*, 121.
(19) Xie, J.; Kaliaguine, S. *Appl. Catal. A* **1997**, *148*, 415.
(20) Gopalakrishnan, S.; Yada, S.; Muench, J.; Selvam, T.; Schwieger, W.; Sommer, M.; Peukert, W. *Appl. Catal. A* **2007**, *327*, 132.
(21) Lippens, B. C.; de Boer, J. H. *J. Catal.* **1965**, *4*, 319.
(22) Groen, J. C.; Jansen, J. C.; Moulijn, J. A.; Perez-Ramirez, J. *J. Phys. Chem. B* **2004**, *108*, 13062.

AM100642W